MONO-ENERGETIC BEAMS FROM LASER PLASMA INTERACTIONS*

C.G.R. Geddes[#§], E. Esarey, C.B. Schroeder, Cs. Toth, J Van Tilborg[†], W.P. Leemans[+], LBNL, Berkeley, California

John R. Cary, CIPS and Tech-X, Boulder, Colorado

Chet Nieter, Tech-X, Boulder, Colorado

Abstract

A laser driven wakefield accelerator has been tuned to produce high energy electron bunches with low emittance and energy spread by extending the interaction length using a plasma channel. Wakefield accelerators support gradients thousands of times those achievable in RF accelerators, but short acceleration distance, limited by diffraction, has resulted in low energy beams with 100% electron energy spread. In the present experiments on the L'OASIS laser, the relativistically intense drive pulse was guided over 10 diffraction ranges by a plasma channel. At a drive pulse power of 9 TW, electrons were trapped from the plasma and beams of percent energy spread containing >200 pC charge above 80 MeV and with normalized emittance estimated at < 2 π-mm-mrad were produced. Data and simulations (VORPAL code) show the high quality bunch was formed when beam loading turned off injection after initial trapping, and when the particles were extracted as they dephased from the wake. Up to 4 TW was guided without trapping, potentially providing a platform for controlled injection. The plasma channel technique forms the basis of a new class of accelerators, with high gradients and high beam quality.

INTRODUCTION

A promising candidate for the next generation of compact high-energy electron sources is the laser wakefield accelerator (LFWA), which has demonstrated accelerating gradients thousands of times those obtained in conventional accelerators using the electric field of a plasma wave (the wakefield) driven by an intense laser[1-3], indicating the potential for more compact accelerators. Acceleration distance and hence electron beam energy and quality has been limited however by the difficulty of retaining high laser intensity over a long distance of propagation in the plasma, resulting in poor quality electron bunches with 100% energy spread and an exponentially small fraction of electrons at high energy [1-3]. Laser power in past experiments was above the critical power for self-focusing and the laser pulse length exceeded the plasma wavelength. In this self modulated regime, some self-guiding of the laser pulse occurs due to relativistic modification of the plasma refractive index, but the laser pulse is highly unstable [4, 5], limiting propagation length to little more than a diffraction range Z_R [6]. The best results had therefore been obtained by increasing spot size to increase Z_R, requiring ever greater laser power, but this approach had still been limited to distances of a few hundred micron [6]. To circumvent this limit and to realize the potential of laser accelerators, the laser pulse should be guided at relativistic intensities, and its propagation controlled over distances of several mm or greater [7].

EXPERIMENT

We report production of high quality electron beams (several 10^9 electrons above 80 MeV energy with percent energy spread and mrad divergence) for the first time in a compact, high gradient, all-optical laser accelerator by extending the interaction distance using a pre-formed plasma density channel to guide the drive laser pulse [8]. The high acceleration gradients of previous laser accelerator experiments are retained over longer distances, and the beam quality is comparable to state of the art RF accelerators. Experiments and simulations showed that the important physics of the new operating regime is that trapping of an initial bunch of electrons loads the wake, suppressing further injection and forming a bunch of electrons isolated in phase space. At the dephasing point, as the bunch begins to outrun the wake, the particles are then concentrated near a single energy, and hence a high quality bunch is obtained by terminating the plasma at this length

Laser guiding at high intensities to produce a channel guided accelerator required compensating both diffraction and plasma effects. Previous experiments demonstrated guiding for input pulse intensities at up to 2×10^{17} W/cm^2 [9-12], where a parabolic transverse plasma density profile can be matched to guide the low intensity pulse [13]. For powers greater than a critical power P_{crit}, relativistic self guiding occurs when the quiver motion of the electrons causes their mass to increase, changing the
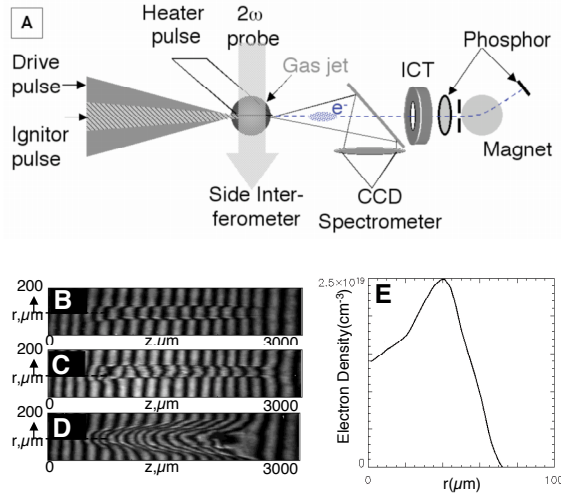
Figure 1. (A) Experimental setup showing the laser beams, gas target, and diagnostics. (B-D) Side interferometer images show the channel structure and laser propagation. At the time of drive pulse arrival (500ps after formation) a channel was formed (B) and the density profile was obtained by Abel inversion (E). Image of the drive beam at 4 TW propagating in this channel (C) is similar to (B) indicating good confinement, while the unguided beam (D) diffracts rapidly.

refractive index. This occurs in regimes of interest to wakefield acceleration and provides some self guiding, but is unstable [4, 5]. The channel must balance both diffraction and instabilities to allow long propagation distance at high intensity.

The multi arm l'OASIS Ti:Sapphire laser [14, 15], operating at 800 nm with chirped pulse amplification, was used to form the guiding channel using a variation of the ignitor-heater method [10] and to drive the plasma wake (Figure 1 A). A plasma was ionized by an ignitor pulse (15mJ, 60fs) from a 2.5 mm long supersonic H_2 gas jet with an atomic density of $3\text{-}4\times10^{19}$ cm^{-3}, then heated to 10's of eV by a heater pulse (using ~50 mJ from a 150 mJ, 250 ps beam). Hydrodynamic expansion of the plasma drove a shock in the surrounding neutral gas, forming a channel with a nearly parabolic transverse density distribution [9]. This channel was used to guide the relativistically intense drive pulse focused at its edge. In order to drive an intense wake capable of trapping and accelerating electrons, the drive pulse (500 mJ, 55 fs) was focused to a spot of 7-8.5 μm FWHM to reach intensities up to 1.1×10^{19} W/cm^2. This gave $Z_R\sim200$ μm so that the channel was $> 10Z_R$ long. Propagation of the laser was monitored with a side interferometer, mode imager CCD, and transmitted light spectrometer. Electrons accelerated by the plasma wake of the drive beam were analyzed using an integrating current transformer (ICT), a phosphor screen, and a magnetic spectrometer.

LASER GUIDING

The channel plasma profile was adjusted to guide the drive pulse at powers up to 2 P_{crit}, and to compensate for the presence of self guiding, by changing ignitor and heater energy and timing [16]. With the channel tuned to match the low power guiding condition [13], aberration free guiding of low power pulses (0.5 TW $< P_{crit}$) was obtained with transmission efficiency of ~50%, but pulses above P_{crit} were aberrated, displaying enlarged output spot size and lowered intensity.

Re-tuning the channel with a reduced density rise allowed compensation for the presence of self guiding, and powers up to 4 TW (7×10^{18} W/cm^2) were guided without aberration. The channel interferogram for this tune at the time of main pulse arrival is shown in Figure 1B. The plasma density profile of the channel (Figure 1E) shows a nearly parabolic transverse dependence, with a rise in density over the spot diameter $\sim 40\%$ less than the low power matching condition. Propagation of the main beam in the channel does not change the image (Figure 1C), indicating that the laser is well confined to the channel, as leakage outside the channel would ionize additional gas. The unguided beam diffracts rapidly, demonstrating that self guiding alone is insufficient to control mode propagation over this distance (Figure 1D).

Figure 2 shows the mode images of the laser spot propagation at 4 TW (7 μm input spot, 7×10^{18} W/cm^2). With the channel on, the output spot (B) matches the input (A). The mode imager resolution is restricted by f/# constraints in the target chamber so that it yields a 12 μm FWHM spot size for both input and output. Deconvolution of instrument response [16] indicated that the output is consistent with a spot within 1 μm of the 7 μm input spot size, giving output intensity $\sim2.5\times10^{18}$ W/cm^2 (lower limit 1×10^{18} set by the 12 μm mode imager observation). The vacuum output displays diffraction (C), indicating the effectiveness of the guide, and with the gas jet on but the channel off (D) diffraction is increased by ionization effects [17, 18], showing that self guiding alone did not efficiently guide the beam.

Transmission at 4 TW was 35 %, a reduction of one third from the low power case, indicating that substantial power was deposited in plasma waves. The depletion observed is consistent with particle in cell simulations run with the experimental parameters (below), which indicate that a plasma wave averaging 2-300 GV/m is excited in the last 0.5 mm of guide length. No electrons are self trapped at 4 TW, making this an attractive structure for controlled injection experiments [19, 20]. Quality and stability of laser accelerated electron bunches may be greatly increased by controlling injection, but such experiments have until now been hampered by lack of a long scale length high gradient structure such as the channel described here can provide. Experiments on colliding pulse injection [20] are now under way in this geometry.

The transmitted spectrum of the laser pulse was also analyzed as a diagnostic of channel confinement and plasma wave excitation. Without the guiding channel, the spectrum showed blue shifting, which occurs when the laser ionizes the gas it is passing through [21]. This
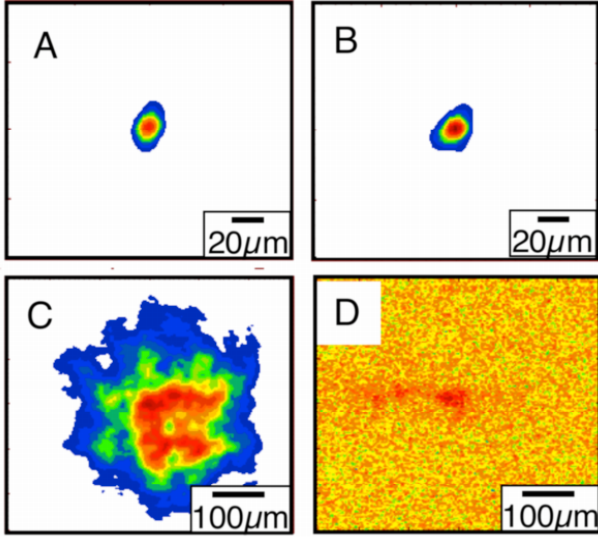
FIGURE 2. Mode images of laser propagation at 4 TW. The output image with the guide on (B) is indistinguishable from the input (A) indicating unaberrated propagation at twice P_{crit}. Unguided images show diffraction in vacuum (C) and ionization enhanced diffraction with the gas jet on (D).

feature was nearly eliminated for the channeled beam, indicating that the laser was well confined to the guiding channel. The spectrum was close to undistorted with transmission of the 800 nm feature near 30% at 4 TW, close to the transmission observed on the mode imager. A red shifted feature appeared in the channeled case, increasing in relative amplitude with laser power, consistent with depletion of the laser into plasma waves.

CHANNELED WAKEFIELD ACCELERATION

At guided drive pulse powers above 4 TW, electrons were trapped and accelerated, verifying that an intense plasma wake was driven in the channel. At 9 TW, optimal performance was found in a channel with an axial density of $1.9 \times 10^{19} \, cm^{-3}$ and with a parabolic profile with 40% less rise in density over a spot diameter than the low power matched case. The laser was well confined to the channel at this power but some aberration was present, with output mode sizes near 24 μm FWHM, likely due to strong self guiding. The drive laser pulse was a factor of two longer than the linear plasma period, in the self-modulated regime. This allowed comparison to unchanneled experiments, and the slower phase velocity of the wake at high plasma density allowed trapping of background plasma electrons, yielding high charge electron beams without a separate injector.

The channel guided accelerator produced high charge electron beams at high energy with low energy spread and low divergence [22]. Figure 3A shows a bunch of 2×10^9 electrons within an energy spread of ±2% centered at 86 MeV. Due to pointing fluctuations which change the incoupling of the drive beam to the guide, this feature

varied shot to shot, and bunches with 3×10^9 electrons at 78 MeV were observed, as well as 1×10^9 electrons at energies up to 150-170 MeV. The charge was calibrated using the ICT and radionuclide activation measurements, which were consistent. Total charge in the electron beam was near 2×10^{10} electrons; the low energy portion can be separated using a bend magnet, leaving a high energy high quality bunch. The divergence of the bunches near 80 MeV was 3 mrad. This is half the divergence of the full beam observed before the magnet (Figure 3B), consistent with other experiments which have shown that the high energy portion of the beam is better collimated [2]. The normalized geometric emittance obtained from assuming the bunch comes from a source ~ the laser spot size is 1-2 π-mm-mrad, competitive with state of the art radiofrequency facilities.
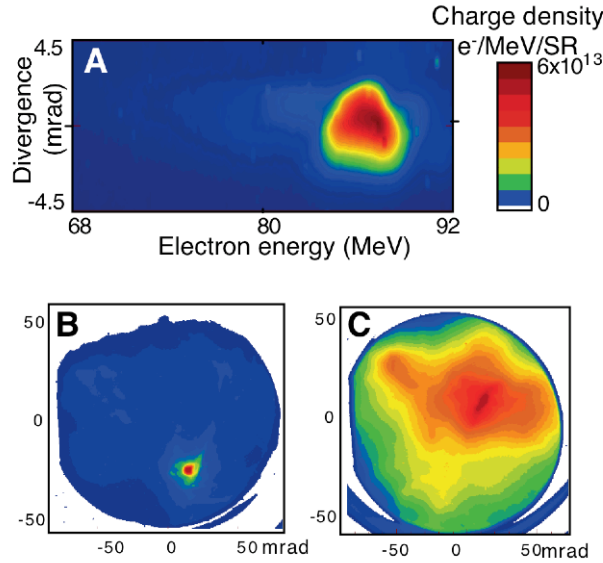

FIGURE 3. Electron bunches. The electron energy spectrum of the channeled accelerator (A) shows the appearance of monoenergetic features, here with 2×10^9 electrons in a bunch with energy spread of 4% FWHM at 86 MeV. Divergence was near 3 mrad FWHM for this bunch (A), and 6 mrad for the whole beam (B). The unguided accelerator in the same gas jet by contrast shows a nearly smooth exponential spectrum with a few MeV temperature (not shown), and wider divergence (C).

The accelerator was operated in the same gas jet without the guiding channel. Density was separately optimized for the unchanneled accelerator and best performance was at $n_e = 4 \times 10^{19} \, cm^{-3}$. This produced an exponential energy distribution with a 2.6 MeV temperature below 10 MeV and an 8 MeV temperature above 10 MeV. No electrons were observed (detection threshold ~ 10^7 electrons on the magnetic spectrometer phosphor) above 40 MeV. The bulk of the distribution was smooth, with occasional structure in the tail of the distribution containing < 2% of the charge. The beam divergence (Figure 3C) was much larger than the channeled case. No difference was observed between operation in a neutral gas jet and a pre-ionized (but not

channeled) plasma, indicating that channeling and not ionization is the important effect.

SIMULATIONS

Two dimensional particle in cell simulations performed with parameters close to the experiment (VORPAL, developed at U. of Colorado/Tech X [23]) indicated that the high quality electron bunches are formed by wake loading and dephasing [8, 24]. If laser pulse strength was just above that required to self trap electrons, loading of the wake [25] by the initial electron bunch trapped suppressed further injection. This lead to a bunch of electrons isolated in phase space (Figure 4). If this bunch was accelerated until it dephased from the wake, the leading edge of the bunch was decelerated while the tail was still accelerating, concentrating the particles in energy and forming a low energy spread bunch at the dephasing length (Figure 4B). Matching accelerator length and dephasing length for the jet length and Z_R used required a guiding channel.
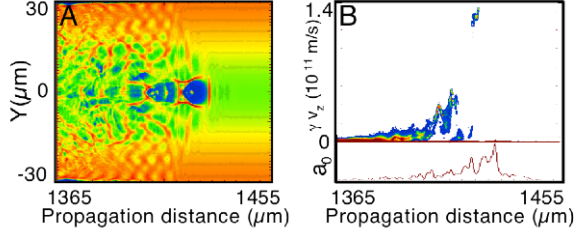

FIGURE 4. Particle in cell simulations show that a high quality bunch is formed when beam loading and pulse evolution turn off injection after the loading of an initial bunch, resulting in an isolated bunch (A). These particles are then concentrated in energy at the dephasing length (B) forming a low energy spread bunch. The laser pulse envelope is shown at the bottom of pane (B), showing self modulation into sub-pulses at the plasma period.

Particles were tracked through the simulation to provide additional information on the particle trajectories (Figure 5). The particles are colored by injection order, with red particles being those injected first (at the shortest propagation distance), and blue last. The particle acceleration trajectories, Figure 5A, verify that bunching in energy occurs when the front of the bunch (first injected particles) decelerates, while electrons at the tail (injected later) continue to accelerate. Beam loading is evident from the reduced slope (dE/dx) of the late injected particle trajectories just after injection. The transverse origin and subsequent behavior of the particles are shown in Figure 5B, indicating that the particles are injected from a radius of approximately 5 μm, rather than from on axis. This reflects the strong ponderomotive blowout by the laser pulse which excludes on axis electrons. A similar effect has also been seen in [26], though in much narrower channels where there was also interaction with the channel-vacuum interface. Formation of quasi-monoenergetic structures was previously observed in [27] at much higher laser amplitudes than those here.
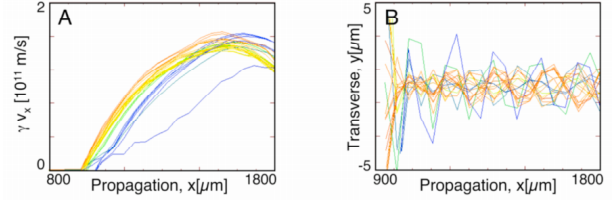

FIGURE 5. Tracks of representative particles in momentum vs. propagation distance (A) and transverse coordinate vs. propagation distance (B).

DEPHASING EXPERIMENTS

To evaluate the impact of dephasing experimentally, gas jets of variable length and density were used without channeling [24]. To meet the dephasing condition without channeling, a short gas jet can be used at the cost of reduced final energy, or self guiding can be used, though this is less stable. PIC simulations were used to evaluate dephasing length, since analytic estimates are not valid in this regime. With the available gas jet lengths and laser Z_R, it was possible to test at and after dephasing at a density of 4×10^{19} cm^{-3}, as well as before and after dephasing at a density of 2×10^{19} cm^{-3}. The electron beam spectra showed that extraction of the beam before dephasing (600 μm plasma at 2×10^{19} cm^{-3}) yielded low energies and a smooth spectrum. Extraction after dephasing (4 mm at 2×10^{19} cm^{-3}, or 2 mm at 4×10^{19} cm^{-3}) produced high energies with some structure in the distribution. The highest energies for a given density, as well as the most monoenergetic features in the spectrum, were obtained when the beam was extracted near the dephasing length (600 μm at 4×10^{19} cm^{-3}). This demonstrates the importance of tuning the accelerator to the dephasing length. Even with such optmization however, the unchanneled accelerator produced less stable, lower quality beams than the channeled accelerator, indicating the advantage of controlling and extending laser propagation length using the channel.

Consistent with the explanation presented here, monoenergetic beams were observed in other experiments using a large laser spot size to increase Z_R and hence the propagation distance of the laser [28, 29]. Like unchanneled experiments herein, this produced less accelerated charge and electron bunch energy per laser power because the large spot size reduced laser intensity, and hence wake amplitude and trapping.

CONCLUSIONS

Experiments have demonstrated guiding of relativistically intense laser pulses over many Z_R in plasmas, and tailoring of the plasma profile to provide guiding without detectable aberration up to twice the relativistic self guiding threshold [16]. Input intensities near 10^{19} W/cm^2 have been guided without self injection of electrons. Increasing density and intensity produced self trapped electron beams of percent energy spread with several 10^9 electrons and with emittance comparable to state of the art radio frequency accelerators [22]. This

offers the possibility of new classes of experiments on laser driven accelerators and indicates that development of high energy high quality beams is feasible using this method, benefiting accelerator applications. Experiments and simulations indicate that these beams are formed by a combination of beam loading and dephasing [24]. Controlled injection using the colliding pulse method [20] will be tried in this structure, which may further stabilize and improve the bunch quality.

REFERENCES

[1] A. Modena, Z. Najmudin, A. E. Dangor, C. E. Clayton, K. A. Marsh, C. Joshi, V. Malka, C. B. Darrow, C. Danson, D. Neely, and F. N. Walsh, Nature 377 (1995) 606.

[2] V. Malka, S. Fritzler, E. Lefebvre, M. M. Aleonard, F. Burgy, J. P. Chambaret, J. F. Chemin, K. Krushelnick, G. Malka, S. P. D. Mangles, Z. Najmudin, M. Pittman, J. P. Rousseau, J. N. Scheurer, B. Walton, and A. E. Dangor, Science 298 (2002) 1596.

[3] W. P. Leemans, P. Catravas, E. Esarey, C. G. R. Geddes, C. Toth, R. Trines, C. B. Schroeder, B. A. Shadwick, J. van Tilborg, and J. Faure, Physical Review Letters 8917 (2002) 4802.

[4] E. Esarey, J. Krall, and P. Sprangle, Physical Review Letters 72 (1994) 2887.

[5] E. Esarey, P. Sprangle, J. Krall, and A. Ting, IEEE Journal of Quantum Electronics 33 (1997) 1879.

[6] Z. Najmudin, K. Krushelnick, E. L. Clark, S. P. D. Mangles, B. Walton, A. E. Dangor, S. Fritzler, V. Malka, E. Lefebvre, D. Gordon, F. S. Tsung, and C. Joshi, Physics of Plasmas 10 (2003) 2071.

[7] E. Esarey, P. Sprangle, J. Krall, and A. Ting, IEEE Transactions on Plasma Science 24 (1996) 252.

[8] C. G. R. Geddes, C. Toths, J. van Tilborg, E. Esarey, C. B. Schroeder, D. Bruhwiler, C. Nieter, J. Cary, and W. P. Leemans, Nature 431 (2004) 538.

[9] C. G. Durfee and H. M. Milchberg, Physical Review Letters 71 (1993) 2409.

[10] P. Volfbeyn, E. Esarey, and W. P. Leemans, Physics of Plasmas 6 (1999) 2269.

[11] K. Y. Kim, I. Alexeev, J. Fan, E. Parra, and H. M. Milchberg, in AIP Conf. Proc., **647**, 646 (2002).

[12] E. W. Gaul, S. P. Le Blanc, A. R. Rundquist, R. Zgadzaj, H. Langhoff, and M. C. Downer, Applied Physics Letters 77 (2000) 4112.

[13] P. Sprangle, E. Esarey, J. Krall, and G. Joyce, Physical Review Letters 69 (1992) 2200.

[14] C. Toth, J. van Tilborg, C. G. R. Geddes, G. Fubiani, C. B. Schroeder, E. Esarey, J. Faure, G. Dugan, and W. P. Leemans, SPIE Proceedings 5448 (2004)

[15] W. P. Leemans, P. Volfbeyn, K. Z. Guo, S. Chattopadhyay, C. B. Schroeder, B. A. Shadwick, P. B. Lee, J. S. Wurtele, and E. Esarey, Physics of Plasmas 5 (1998) 1615.

[16] C. G. R. Geddes, C. Toth, J. van Tilborg, E. Esarey, C. B. Schroeder, and W. P. Leemans, Submitted to Phys. Rev. Lett., 2004.

[17] R. Rankin, C. E. Capjack, N. H. Burnett, and P. B. Corkum, Optics Letters 16 (1991) 835.

[18] W. P. Leemans, C. E. Clayton, W. B. Mori, K. A. Marsh, P. K. Kaw, A. Dyson, C. Joshi, and J. M. Wallace, Physical Review A. Atomic, Molecular, and Optical Physics 46 (1992) 1091.

[19] D. Umstadter, J. K. Kim, and E. Dodd, Physical Review Letters 76 (1996) 2073.

[20] E. Esarey, R. F. Hubbard, W. P. Leemans, A. Ting, and P. Sprangle, Physical Review Letters 79 (1997) 2682.

[21] E. Esarey, G. Joyce, and P. Sprangle, Physical Review E. Statistical Physics, Plasmas, Fluids, & Related Interdisciplinary Topics 44 (1991) 3908.

[22] C. G. R. Geddes, C. Toth, J. van Tilborg, E. Esarey, C. B. Schroeder, D. Bruhwiler, C. Nieter, J. Cary, and W. P. Leemans, Nature 431 (2004) 538.

[23] C. Nieter and J. R. Cary, Journal of Computational Physics 196 (2004) 448.

[24] C. G. R. Geddes, C. Toth, J. van Tilborg, E. Esarey, C. B. Schroeder, D. Bruhwiler, C. Nieter, J. Cary, and W. P. Leemans, Physics of Plasmas 12 (2005) 056709.

[25] T. Katsouleas, S. Wilks, S. Chen, J. M. Dawson, and J. J. Su, Particle Accelerators 22 (1987) 81.

[26] F. S. Tsung, N. Ritesh, W. B. Mori, C. Joshi, R. A. Fonseca, and L. O. Silva, Physical Review Letters 93 (2004) 1.

[27] A. Pukhov and J. Meyer-Ter-Vehn, Applied Physics B Lasers & Optics (2002) 4.

[28] J. Faure, Y. Glinec, A. Pukhov, S. Kisetev, S. Gordienko, E. Lefebvre, J. P. Rousseau, F. Burgy, and V. Malka, Nature 431 (2004) 541.

[29] S. P. D. Mangles, C. D. Murphy, Z. Najmudin, A. G. R. Thomas, J. L. Collier, A. E. Dangor, E. J. Divall, P. S. Foster, J. G. Gallacher, C. J. Hooker, D. A. Jaroszynski, A. J. Langley, W. B. Mori, P. A. Norreys, F. S. Tsung, R. Viskup, B. R. Walton, and K. Krushelnick, Nature 431 (2004) 535.